

North Sea Energy

Technical assessment of Hydrogen transport, compression, processing offshore

As part of Topsector Energy:
TKI Offshore Wind & TKI New Gas

Prepared by: TNO: Néstor González Díez
TNO: Simone van der Meer
EDI: Jorge Bonetto
HINT: Arend Herwijn

Checked by: TNO: Carey Walters, Stefan
Belfroid, Joris Koornneef

Approved by: TNO: Madelaine Halter
NSE coordinator

Table of Contents

1	Executive summary	3
2	Introduction.....	4
	Objectives of the analysis	4
	Scope of the analysis.....	4
	Equipment in contact with hydrogen	4
	Structure of the report	5
3	Offshore pipelines: impact of H ₂	6
	Hydrogen export routes	6
	Offshore Pipeline Construction	11
	Hydrogen flow in pipelines	11
	Risks related to hydrogen injection	14
	Fatigue	15
	Outlook.....	20
4	Compressors: impact of H ₂	22
	Reciprocating compressors	22
	Centrifugal compressors	22
	Costs of refurbishing a compressor system for hydrogen duty	23
	Outlook.....	25
5	Gas engines and gas turbines: impact of H ₂	26
	Gas engines: impact of Hydrogen additions	26
	Gas turbines: impact of Hydrogen additions.....	26
6	Flow meters: impact of H ₂	27
	Literature survey	27
	Input supplied by vendors	29
7	References	30

1 Executive summary

The North Sea has an opportunity to play a new role in decarbonising both the energy and industrial sectors. The simultaneous decline of oil & gas production and increase in offshore wind generation creates an opportunity for oil & gas infrastructure to be repurposed via power-to-gas technology.

In the context of North Sea Energy 3, WP 3.3. *Technical assessment of Hydrogen transport, compression, processing offshore*, the question on the re-use of infrastructure is addressed in further detail. In this WP, the main objective is to investigate the acceptability of hydrogen in the existing infrastructure. This can be broken down into the following questions:

- Can the existing equipment be re-used for hydrogen service?
- What are the admissible concentrations of hydrogen for the equipment expected to be in contact with hydrogen?
- What would be the costs of adopting measures to address the barriers or showstoppers found in any of the questions above?

A generic investigation based on existing, available literature is done for the hardware expected to be in contact with hydrogen (or blends of natural gas hydrogen):

- Offshore pipelines
- Compression equipment
- Gas turbines and engines
- Flow metering
- (out of scope of this report) Valves and other flow fittings.

Pipelines have been investigated regarding the compatibility between the natural gas/hydrogen mixture and the material properties. The focus is placed on the influence of hydrogen on the fatigue properties of relevant steel grades and the resulting crack propagation. No showstoppers have been identified. No significant effects due to hydrogen-enhanced fatigue crack growth are expected for the typical offshore operating conditions and material types (X42-X70). It is important to note that the current condition of the integrity of the pipelines has not been assessed in this investigation. Therefore, the results contained in this report should be combined with the results of an inspection, that determines whether defects exist and whether those match the assumptions taken in this investigation.

In a future service for the North Sea infrastructure in which hydrogen is to play a role, compressors will continue to be at the heart of the export system. Concentrations up to 10%vol of hydrogen have been claimed to be acceptable in existing mechanical compressors. Besides operation and performance, particular attention must be given to material compatibility and fugitive losses through the seals. The costs of replacement can be elevated. To boost the amount of hydrogen produced in a current proton-exchange membrane (PEM) electrolyser to export pressure, compression CAPEX is roughly estimated at 25 kEUR/(MW_electrolyzer_input). The OPEX is approximately one quarter of that on a yearly basis (~ 6.5 kEUR per annum per MW of electrolyzer input).

Engines and turbines can be sensitive to hydrogen additions. Gas engines can run into engine knocking difficulties at small hydrogen concentrations, and adapting to the fluctuations of the hydrogen level can be a challenge. For gas turbines, power output, emissions and flame stability can be an issue.

Flow meters are impacted by the presence of hydrogen in different ways depending on the measuring principle of the meter. While turbines and ultrasonic flow meters currently have a hard limit on maximum flow velocity and measurable flow range, coriolis flow meters are and can be used for hydrogen. Nevertheless, issues remain regarding the lack of metrological approval for meters used in 100% hydrogen. Finally, the function of the meter alone (billing) is insufficient when the gas composition is rapidly fluctuating. Gas chromatographs or alternative gas composition sensors must be developed for high hydrogen concentrations.

2 Introduction

The North Sea has an opportunity to play a new role in decarbonising both the energy and industrial sectors. As more offshore wind comes online in the following decades, power-to-gas (P2G) technology has been identified as an enabler to an accelerated energy transition. Power-to-gas technology considers the conversion of electrical power generated in wind parks into hydrogen as an energy carrier, via water electrolysis.

At the same time that the capacity of offshore wind is planned to increase, oil and gas production is following the inverse trend: reservoirs are reaching depletion, pipelines have capacity available and assets are being decommissioned. Existing infrastructure could be used as an instrument for system integration in the North Sea. The offshore platforms can be used as hosts for P2G conversion and the pipelines can be used to transport the (chemical) energy to shore.

In the context of North Sea Energy 3, WP 3.3. *Technical assessment of Hydrogen transport, compression, processing offshore*, the question on the re-use of infrastructure is addressed in further detail.

Objectives of the analysis

The main objective of the research is to investigate the acceptability of hydrogen in the existing infrastructure. This can be broken down into the following questions:

- Can the existing equipment be re-used for hydrogen service?
- What are the admissible concentrations of hydrogen for the equipment expected to be in contact with hydrogen?
- What would be the costs of adopting measures to address the barriers or showstoppers found in any of the questions above?

Scope of the analysis

Because analyzing every specific piece of existing equipment is of course beyond the scope of this work package, a generic investigation based on existing, available literature is done. The prioritization on what part of the offshore infrastructure is analysed is based on the expected costs of the equipment itself:

- Offshore pipelines
- Compression equipment
- Gas turbines and engines
- Flow metering
- Not in scope: valves and other flow fittings

Equipment in contact with hydrogen

In order to make an inventory of the type of equipment that will be in contact with the hydrogen produced via electrolysis, it has been assumed that this process coexists with the hydrocarbon production process (Figure 1). This is the possibility in which hydrogen comes into contact with the most types of equipment. It is a scenario representative of possible pilots happening in the next 5 years.

In this scenario, hydrogen produced in a PEM¹ unit would be at a sufficient pressure to be injected upstream of the export compressor (in cases with free-flow operation, one can eliminate the compressor and driver from this overview). After being compressed, a portion of the gas is fed to a gas-fired prime mover, such as a gas turbine or a gas engine. The majority of the gas is directly exported via export pipeline², which downstream may merge into a larger export trunkline. A possible two-phase flow mixture between in the

¹ The type of electrolysis technology chosen in this WP is actually not entirely relevant. Here PEM is mentioned purely due to its reduced footprint compared to alkaline technology and thus more realistic possibility in case of coexistence with the regular production process.

² It is possible, depending on the actual conditions of an asset, that the gas (combined with hydrogen) is mixed with the liquid stream into a single flowline. This possibility is excluded in the scope of this WP.

trunklines, including natural gas, hydrogen, liquid condensates and free water is not investigated in this research.

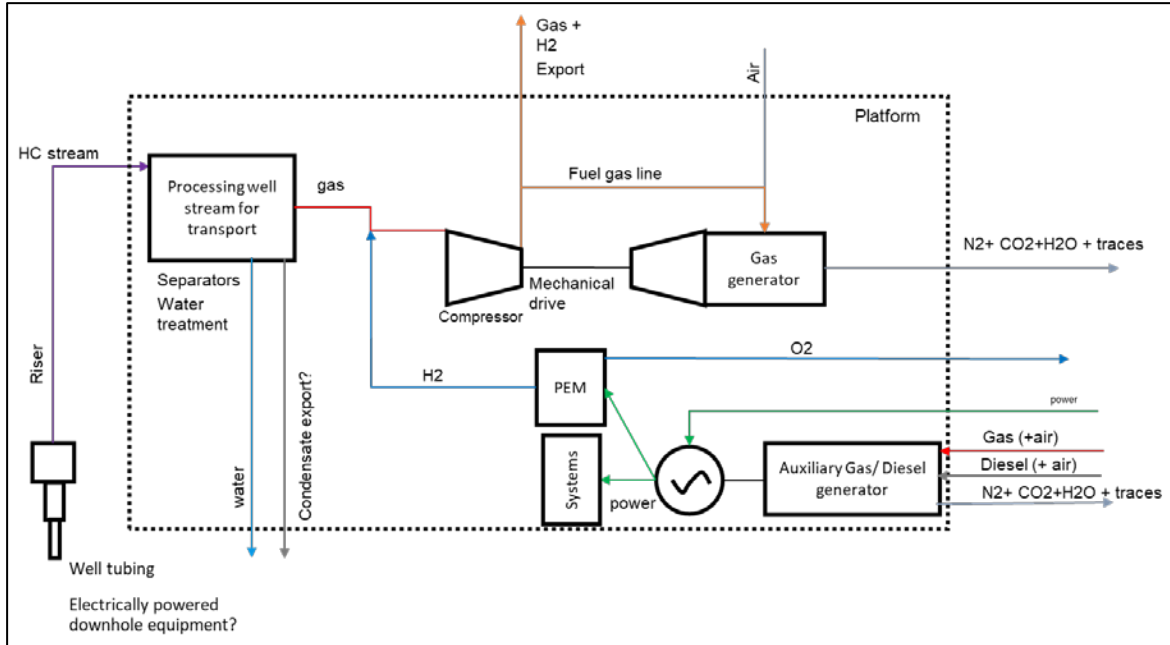


Figure 1. Assumed layout of a platform. In the most generic possibility, the new process (P2G) coexists with the normal hydrocarbon production process.

Structure of the report

The report is structured according to the inventory of equipment in contact with H₂ presented above. First, the offshore export pipelines are looked at in detail and with higher priority, followed by the study regarding compressors. Primer movers such as engines and turbines are investigated next, and finally, flow meters are analysed. Other equipment such as valves and flanges is left outside the scope of this report, though it is expected to be generated still within the context of NSE 3.

3 Offshore pipelines: impact of H₂

In this chapter, the admissible concentration of hydrogen in existing pipelines is investigated. First, an overview of the offshore pipelines potentially available for hydrogen transport is given. With this information, the features of the pipelines are known, and thus a systematic analysis of their re-use challenges can be done. This analysis is based on one hand on the aspects related to the flow of hydrogen (or blends of hydrogen and natural gas) and, on the other, the aspects related to the integrity of the pipeline.

Hydrogen export routes

The aim of this section is to provide a first selection of potential routes for transporting hydrogen volumes produced offshore at the Dutch continental shelf (DCS) in the North Sea to a destination or delivery point onshore. Making use of the NSE 1 results – namely the North Sea Energy Atlas [1] – and the selection of consumption regions being used in the work package 1.5 from NSE 3 (see Figure 2), a first selection of available and existing pipeline infrastructure was selected.

The consumption regions are characterized by their future potential demand as foreseen within the climate agreement outlined in ref. [2] and further detailed in ref. [3].

Selection criteria

In order to make an inventory of the most interesting export routes for hydrogen, existing pipelines and trunk lines were chosen according to their level of alignment to the following criteria: location of potential hydrogen production regions, location of potential hydrogen demand regions, and what the expected developments for the pipelines in the coming decades are. Eventual use of the pipelines for CO₂ transport and storage is possible, but excluded from this evaluation.

1. Location of concentrated production

This parameter takes into consideration the potential future locations of hydrogen production in the North Sea. These locations will determine the starting point from where the volumes of hydrogen will need to be injected into the existing pipeline.

Based on the PBL - Rapid Development Scenario [4], the most promising locations will be Hollandse Kust, IJmuiden Ver, Doggers Bank and the Cleavers Bank.

- *Hollandse Kust*
A Wind Farm Zone composed of 4 sites off the west coast of the Netherlands, in the coastal waters of the province of Zuid-Holland. If hydrogen was to be produced in this area, the following existing gas pipelines could be used³:
 - TAQA 26-inch running from platform P15 to shore at Maasvlakte, with a potential flow rate of 111 tonsH₂/h.
 - A system composed of the TAQA 16-inch, GDF Suez 8-inch and NAM 8-inch gas pipelines, running from platform P15 to shore at Maasvlakte, with a combined potential flow rate of 60 tonsH₂/h.
- *IJmuiden Ver*
A 4 GW Wind Power capacity is planned to become operative by 2030, which could be used partly or entirely for the production of hydrogen:
 - WGT 36-inch gas pipeline running from platform K13 to Den Helder, with a potential hydrogen flow rate of 220 tonsH₂/h.
 - LOCAL 24-inch gas pipeline running from platform K15 to Den Helder, with a potential hydrogen flow rate of 95 tonsH₂/h.
 - NGT 36-inch gas pipeline running from platform K12/L10 to Eemshaven, with a potential hydrogen flow rate of 220 tonsH₂/h.

³ All capacities quoted here are based on transport at 80 bar and 15 m/s flow speed, pure hydrogen flow.

- **Doggers Bank**
An energy hub at the Doggers Bank area is a possibility currently considered, mainly due to its attractiveness given by its location far away from shore that prevents complaints about visual impacts, and also for the shallow waters which allows a traditional foundation for the wind turbines. Nevertheless, there are no accurate estimations on the amount of wind power capacity that will be installed, but still is considered as a potential future hydrogen production location. Given the scenario that large volumes of hydrogen would have to be exported from this area to shore, the following existing gas infrastructure shows the most significant potential to do so:
 - NOGAT 24-inch gas pipeline running from platform L2 to Den Helder, with a potential flow rate of 95 tonsH₂/h.
 - NGT 36-inch gas pipeline running from platform L10 to Eemshaven, with a potential hydrogen flow rate of 220 tonsH₂/h.

- **Cleavers Bank**
This area is primarily considered as a protected nature area, but the PBL studies nevertheless predict a potential for energy parks to be developed. Therefore, hydrogen export routes reusing the existing gas infrastructure would consist of the following trunk lines:
 - NGT 36-inch gas pipeline running from platform K12/L10 to Eemshaven, with a potential hydrogen flow rate of 220 tonsH₂/h.
 - WGT 36-inch gas pipeline running from platform K13 to Den Helder, with a potential hydrogen flow rate of 220 tonsH₂/h.
 - WGT 24-inch gas pipeline running from platform J06 to Den Helder, with a potential hydrogen flow rate of 95 tonsH₂/h.

2. Location of concentrated demand

A selection of routes is made by filtering the existing gas pipelines that converge towards the consumption sectors at shore identified in NSE3 WP 1.5, which are shown and depicted with roman numbers (from I to IV) in Figure 2.

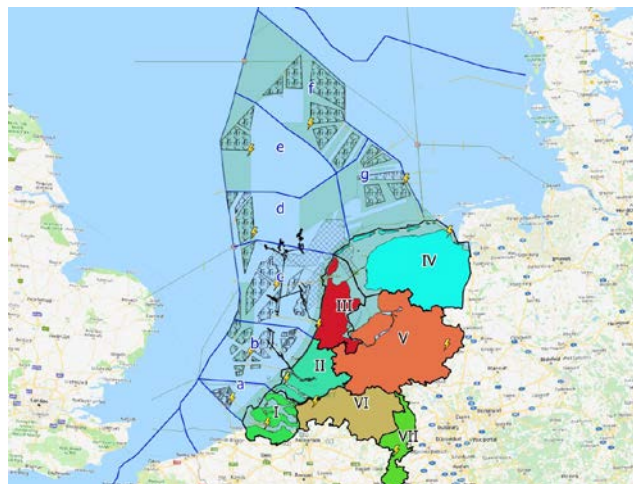


Figure 2. Hydrogen consumption sectors as envisioned in NSE 3 WP 1.5

- **Sector I**
Referred as the Zeeland region, this sector presents a total demand of 2,249 MW of hydrogen in the year 2050 according to the medium scenario [2]. With regards to the offshore existing gas infrastructure converging to this particular area, there are no trunk-lines available to be considered.

- Sector II**

This sector is referred to as the Rotterdam region in NSE3 WP 1.5 and presents a total demand of 9,474.16 MW of hydrogen in the year 2050 according the medium scenario [2]. In Figure 3 below, the two potential export routes are highlighted in yellow and green, the former being composed by an existing interconnection of three pipelines, and the latter is the TAQA header going to Maasvlakte. Table 1 presents the pipelines converging to this sector, and the ones designed for gas transport (and perhaps also hydrogen) are highlighted in bold font.
- Sector III**

This sector is referred to as the IJmuiden region in NSE3 WP 1.5 and presents a total demand of 2,948.6 MW of hydrogen in the year 2050 according the medium scenario [2]. Despite the fact that a large number of transport lines converge to this sector, only four of them are currently used for gas transport. The BBL pipeline (36-inch) runs from the Dutch shore to the UK shore, with no intermediate platforms nor potential tie-in. Therefore this line is less suitable. For the Chevron (20-inch) and Wintershall (12-inch) lines, these are currently designed for oil transportation and, consequently, not best suited for gaseous delivery. The potential export routes using existing pipelines in this region are depicted in Figure 4, and the details of these trunk-lines are listed in Table 2.
- Sector IV**

This sector is referred to as the Eemshaven region in WP 1.5 and presents a total demand of 3,962.68 MW of hydrogen in the year 2050 according the medium scenario [2]. In this region, the NGT trunk-line is the only available gas pipeline.

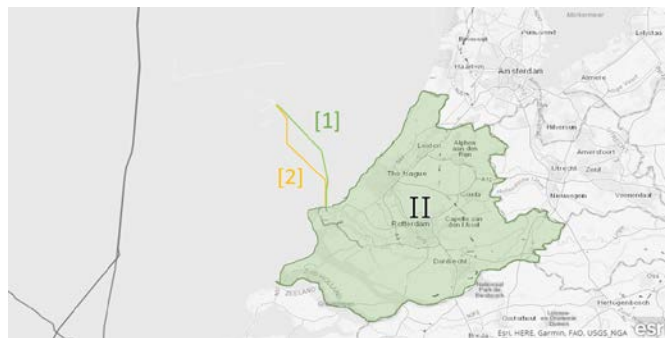


Figure 3. Sector II potential export routes

Table 1. Offshore pipelines converging in Sector II

Name	Operator	Diameter [in]	Fluid	Tie-in	End
PL0039_PR	TAQA Energy B.V.	10	Oil	P15-C	Hoek van Holland
PL0099_PR	TAQA Energy B.V.	26	Gas	P15-D	Maasvlakte
PL0223_PR	GDF SUEZ E&P Nederland B.V.	8	Gas	Q16-FA-1	Maasvlakte
PL0138_PR	NAM	8	Gas	Q16-FA-1	P18-A
PL0106_PR	TAQA Energy B.V.	16	Gas	P18-A	P15-D
PL0228_PR	GDF SUEZ E&P Nederland B.V.	8	Oil	P15-C	Q13a-A
PL0138_HS	NAM	2	Methanol	Q16-FA-1	P18-A

Table 2. Offshore pipelines converging in Sector III

Name	Operator	Diameter [in]	Fluid	Tie-in	End
PL0030_PR	NAM	24	Gas	K15-FB-1	LOCAL
PL0176_PR	BBL Company V.O.F.	36	Gas		Balgzand
PL0004_PR	Wintershall Noordzee B.V.	36	Gas	K13-AP	WGT
PL0091_PR	GDF SUEZ E&P Nederland B.V.	24	Gas	L2-FA-1	NOGAT
PL0025_PR	Chevron Exploration	20	Oil	Q1-Helm-AP	Ijmuiden
PL0061_PR	Wintershall Noordzee B.V.	10.7	Gas	Q8-A	Ijmuiden
PL0218_PR	Wintershall Noordzee B.V.	10	Gas	Q4-C	Q8-A
PL0038_PR	Wintershall Noordzee B.V.	12	Oil	K18-Kotter-P	Q1-Helder-A

Table 3. Offshore pipelines converging in Sector IV

Name	Operator	Diameter [in]	Fluid	Tie-in	End
PL0003_PR	Noordgastransport B.V.	36	Gas	L10-AR	NGT
PL0142_PR	Noordgastransport B.V.	36	Gas	D15-FA-1	L10-AC

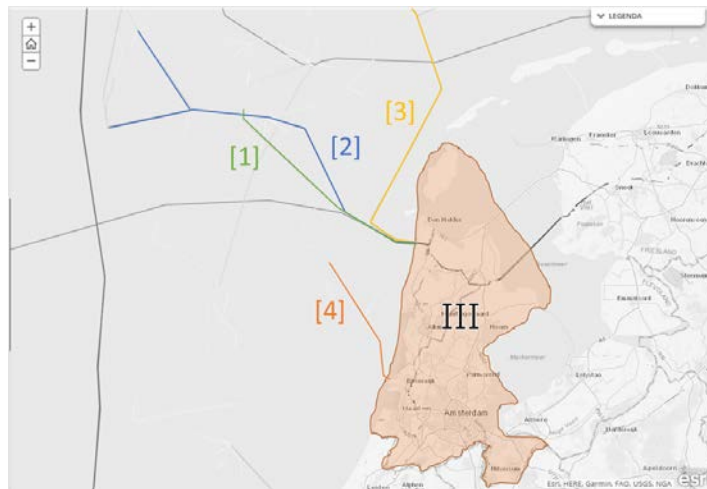


Figure 4. Sector III potential export routes

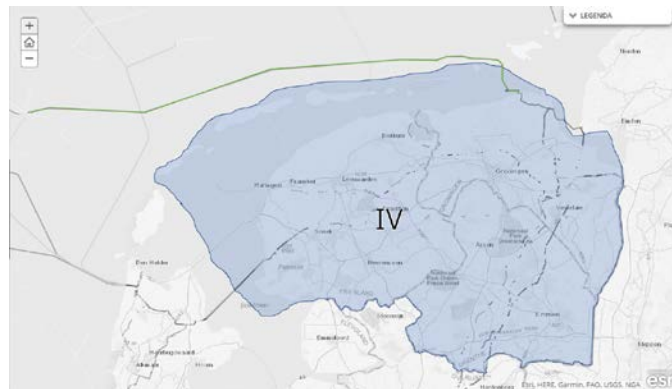


Figure 5. Sector IV potential export routes.

3. Future developments

A consideration must be made in terms of timing when assessing the potential routes. The reason for this criterion lies on the decreasing production of natural gas targets set by the Dutch authorities. This will reflect on the possibilities of re-using the existing infrastructure for transportation of pure hydrogen flow or a blend of natural gas and hydrogen.

The readiness of the existing infrastructure will be given by the decommissioning or end-of-production date of each of the platforms. This information is not sufficiently available yet to make a full assessment and far from certain: therefore, the study could take into account the following estimation made by EBN⁴ with regards to the estimated throughput of the trunklines for the upcoming years. With current information, one may assume 15 mln Nm³/day in 2020 with a linear decline until 2040 of 2 mln Nm³/day. Predictions after 2040 are even more uncertain.

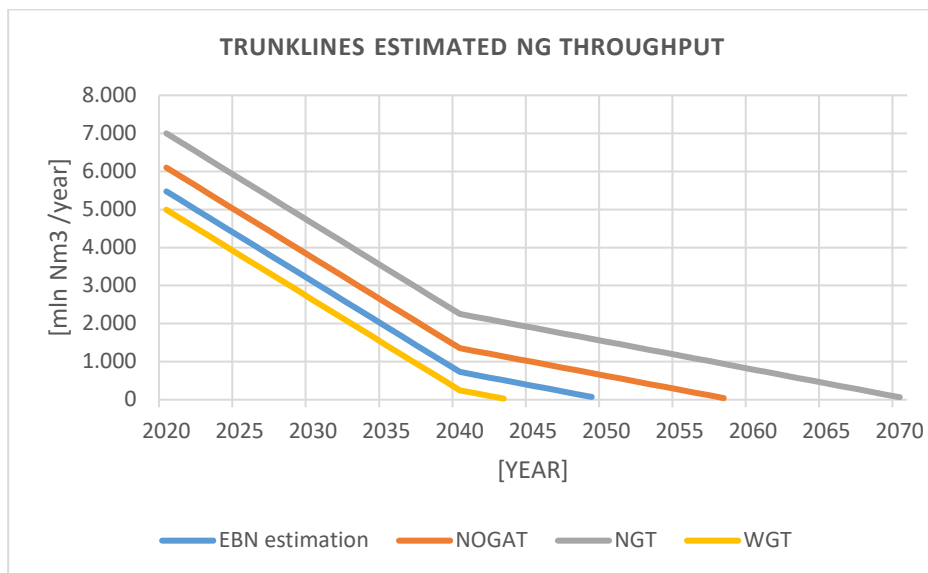


Figure 6. Forecast of natural gas transport volumes as a function of time, for three of the largest offshore pipelines in the North Sea.

Summary

The inventory of pipelines identified for potential re-use with hydrogen (or blend with natural gas) is given in Table 4.

⁴ Information shared through email exchange with EBN within the context of the developing the research study [5]

Table 4. Inventory of identified pipelines potentially attractive to transport hydrogen.

Pipe segment	Operator	NPS [inches]	Duty	From...	To...
PL0099_PR	TAQA	26	Gas	P15-D	Maasvlakte
PL0223_PR	Neptune	8	Gas	Q16-FA-1	Maasvlakte
PL0138_PR	NAM	8	Gas	Q16-FA-1	P18-A
PL0106_PR	TAQA	16	Gas	P18-A	P15-D
PL0030_PR	NAM	24	Gas	K15-FB-1	LOCAL
PL0004_PR	Wintershall	36	Gas	K13-AP	WGT
PL0091_PR	Neptune	24	Gas	L2-FA-1	NOGAT
PL0061_PR	Wintershall	10.7	Gas	Q8-A	Ijmuiden
PL0218_PR	Wintershall	10	Gas	Q4-C	Q8-A
PL0003_PR	Noordgastransport	36	Gas	L10-AR	NGT
PL0142_PR	Noordgastransport	36	Gas	D15-FA-1	L10-AC

Offshore Pipeline Construction

Offshore trunk pipelines in the North Sea have been developed from the 1970's up to the late 1990's. In general, they are made of carbon steel grades X42 through to X70, with longitudinal welds. This is in line with the typical materials selected in European countries at the time (Figure 7, ref. [5]). Outer diameters vary per segment, whereas the schedule is typically XS or thicker (> 12.7 mm).

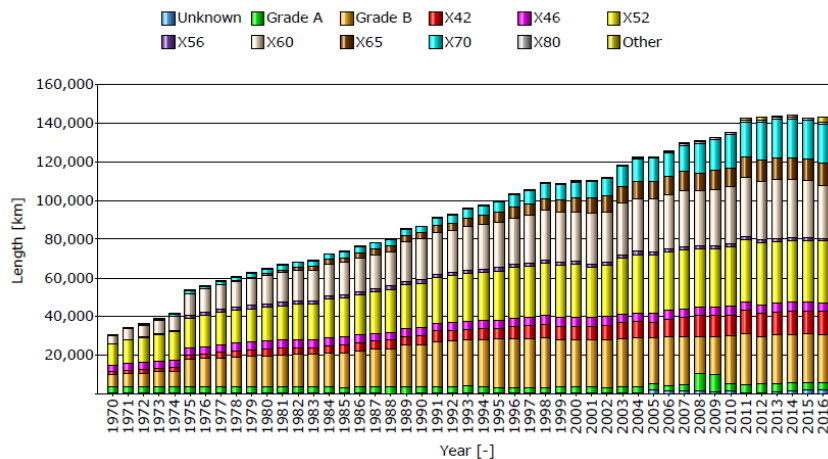


Figure 7. Steel grade selection as a function of pipeline installation year and cumulative length. This information refers to all of Europe, without taking into consideration onshore or offshore conditions. (Obtained from ref. [5]).

Hydrogen flow in pipelines

The energy locked in the chemical bonds of diatomic hydrogen (H₂) can be transported via pipeline. The energy density of hydrogen is low compared to natural gas. Therefore, when re-using pipelines, it is important to determine what the export capacity of the pipeline is, if it is to be re-purposed for hydrogen duty or a mixture of natural gas and hydrogen. In this section, this is explored from a general perspective. In particular, the following sensitivities are explored:

- Pipeline size
- Operating pressure
- Hydrogen concentration

In the general discussion, the flow rates are calculated at a given reference point (e.g. pipeline outlet). Several choices have been made:

- Pipeline outer diameter follows ASME Nominal Pipe Size (NPS) standard.
- Wall thickness assumes Schedule XS for all sizes considered.
- Pipeline surface roughness 100 μm (equivalent sand grain).
- Temperature of 10 deg. C⁵.
- Flow speed of 15 m/s⁶.
- Energy content is based on a high heating value (HHV) of 141.9 MJ_{th}/kg.

The transport capacity of a pipeline is depicted in Figure 8. This plot shows that the capacity for a pipeline to transport energy is substantial, especially if the typical sizes and design pressures of offshore pipelines is considered. For example, if one would assume that the plans for 2023 regarding offshore wind in the Netherlands were to be achieved (4500 MW installed capacity) and that the windfarms would be producing at capacity *all* year round, *all* power converted into hydrogen would fit in a 20-inch pipe operating at 80 bar(a).

The estimated pressure drop for the conditions summarized above is depicted in Figure 9. These values are in line from what would be expected in a typical North Sea line, which is 3-10 bar/100km [6], though higher values up to 25 bar/100km are not considered unusual [7].

Regarding blends of natural gas and hydrogen, the energy transport capacity (at 80 bar) is reduced by a maximum of 25% if the same pressure drop is to be maintained (Figure 10), which is achieved at concentrations between 70% and 90%mol for G-gas and H-gas, respectively.

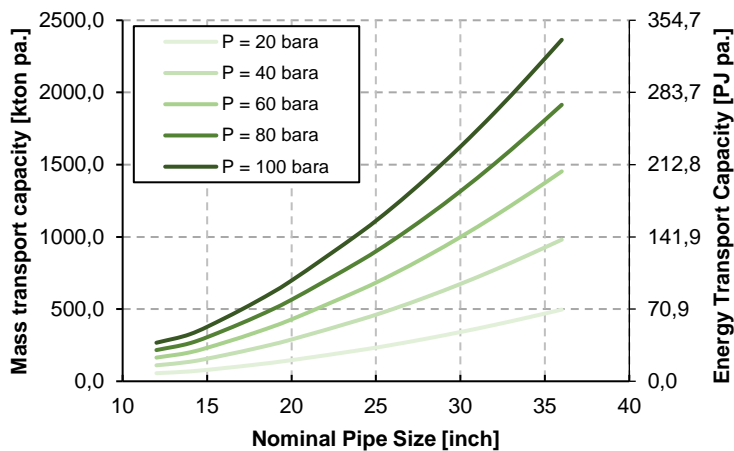


Figure 8. H₂ transport capacity of hydrogen pipeline and equivalent annual energy export capacity, as a function of size and operating pressure.

⁵ A temperature of 10 deg. C corresponds approximately to the North Sea annual average temperature [42]. Therefore, it is assumed that the reference point is in thermal equilibrium with the environmental temperature.

⁶ This is selected as a safe, maximum value that ensures that flow velocities at eventual processing facilities remain below an upper limit of 20 m/s. The flow speed itself may be constrained on a maximum pressure drop resulting from a compressor selection based on the most economic scenario. In any case, the pressure drops are calculated and typically in the range of 10-20 kPa/km.

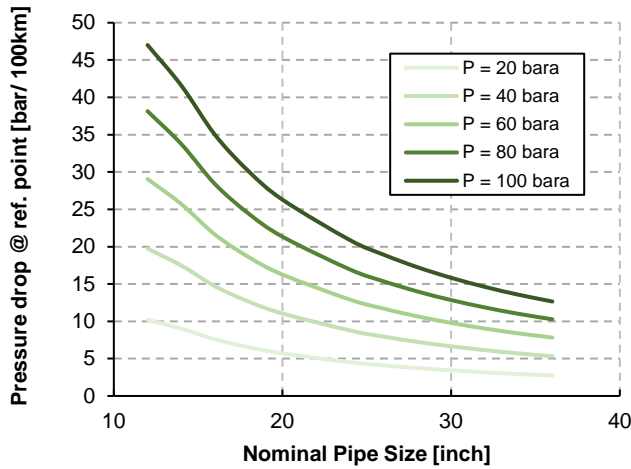


Figure 9. Pressure drop at a given reference point for different operating pressures, all at 15 m/s and therefore at different flow rates (as shown in previous Figure 8).

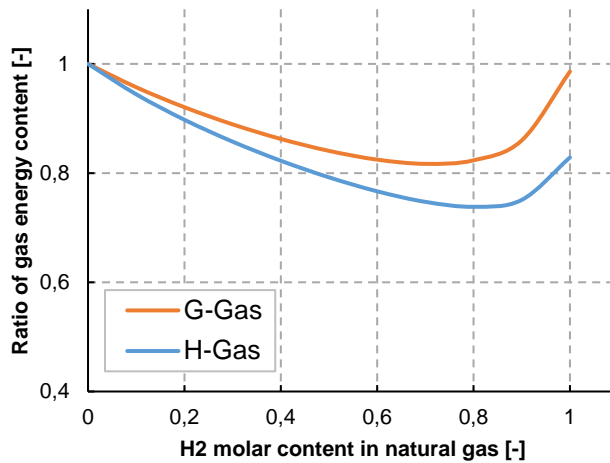


Figure 10. Ratio of energy content in a blend of natural gas and hydrogen, for Groningen gas (G-gas) and high calorific gas (H-gas), for different concentrations of H₂, to maintain *pressure drop constant*. Pressure is assumed to be 80 bar.

Maximum flow velocity in pipelines

One of the main assumptions in the previous analysis regarding the calculation of pipeline capacity is the assumed flow velocity. For a new project, flow velocity, pipeline pressure, pipeline diameter, number of compressors, their locations and power are the result of cost optimization. For the North Sea, considering the potential re-use of existing pipelines and assets, it is possible to assume a particular flow velocity by selecting suitable compressors. The flow velocity assumed in the previous analysis is 15 m/s. This number could be increased if it was acceptable from the following perspectives:

- Flow-induced vibration
- Erosion
- Instrumentation such as thermowells and flow meters (see chapter 6)

According to ref. [8], increasing the flow velocity for higher concentrations of hydrogen is possible from flow-induced turbulence (Figure 11) and flow-induced pulsations perspective. However, intrusive elements such as thermowells and some types of flow meters can experience a larger risk of failure when exposed to higher

flow velocities, even at similar levels of flow kinetic energy. For clean, dry gas systems, velocity limitations are determined by pressure drop and vibration/noise limitations⁷.

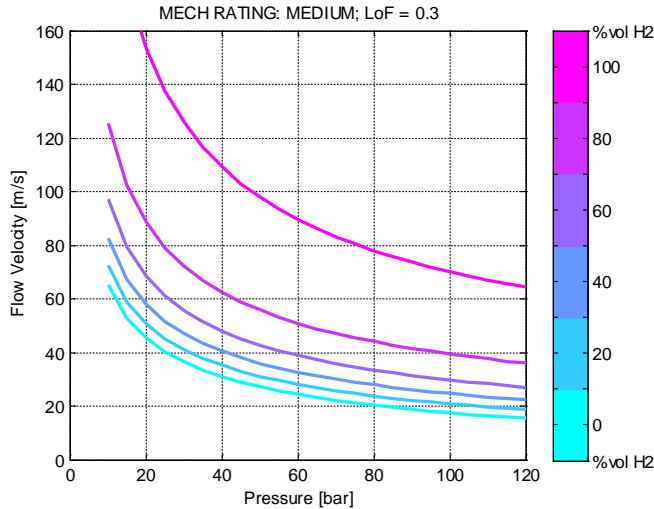


Figure 11. Allowable flow velocity to achieve a Likelihood of Failure score of 0.3 (risk acceptable, no actions required), following Energy Institute Guidelines [9], regarding flow-induced turbulence only. Values are calculated for flow at 0°C and a 36" (DN900) header with schedule XS, with a mechanical supporting layout deemed as MEDIUM.

Risks related to hydrogen injection

When introducing hydrogen in the natural gas stream or the stream is of pure hydrogen, the material of the pipeline will be affected by the potential diffusion of hydrogen through the metal.

On the current condition of the integrity of the pipelines

In the scope of this project and the analysis to follow, the considerations on material compatibility are made purely from a design perspective. The current condition of the integrity of the pipelines are however equally important. After decades of operation, in some cases with two-phase flow mixtures, initial defects due to corrosion may exist, which may be activated by the presence of hydrogen. A crucial recommendation is to execute a pipeline inspection with suitable inspection technology to determine if anomalies are present and to size them. Reference [10] provides a current overview of inspection techniques available to this end.

Change in plasticity of the steel grades

Offshore pipelines can be subject to several internal and external loads, which can be both static and dynamic. For example, it is well known that the mobility of the soil can lead to long unsupported spans resulting in large static loads (for self-buried pipes). It can also be dynamically loaded by (external) vortex-induced vibration related to the underwater currents. The pipeline can also be hit by external objects. All external loading factors will be the same regardless of whether or not hydrogen flows inside the pipeline; however, the resistance to them may be affected by the presence of hydrogen. It is therefore essential to determine whether the typical mechanical properties of the material are severely affected by the presence of hydrogen.

Reference [11] from Sandia National Labs is a widely used summary, updated when necessary, of investigations related to the compatibility of materials to hydrogen. Interestingly, information available for

⁷ Regarding erosion, the limits may be the same for natural gas and hydrogen, since eventual solid particles will be dragged by the flow above a minimum flow velocity. Note that API 14E [43] or NORSOK P-001 suggest a limit inversely proportional to the square root of the stream mixture density, which would be in the benefit of higher hydrogen concentrations in the gas stream. Its applicability to dry gas + solid mixtures is still unclear.

X42-X70 is available for atmospheres of hydrogen at 69 bar, which is approximately the operational pressure in an offshore pipeline. The effect of hydrogen at 69 bar on the mechanical properties of the material is shown in Table 5. It is observed that the differences are minor and can be accepted.

Table 5. Variation in basic material mechanical properties in the presence of H₂.

% variation with H ₂ @ 69 bar, room temperature, vs air*	X42	X52	X60	X65	X70
Yield Strength	-9.6	3.6	-1.2	0.4	-6.2
Tensile Strength	-5.5	-2.0	-0.7	1.0	-1.5
Elongation at fracture	-4.8	-21.1	-23.1	0.0	0.0

(*) Note that strain rate is applied either at $1 \times 10^{-4} \text{ s}^{-1}$ or $\sim 3 \times 10^{-4} \text{ s}^{-1}$, depending on the case.

Corrosion

Corrosion can either initiate from the outer side or the inner side of the pipe. External corrosion in a submarine environment will remain the same regardless of the presence of hydrogen. Besides the loss of pipe wall thickness (uniform corrosion), corrosion creates (pitting corrosion) defects on which cracking can develop due to tensile stress, eventually leading to leakage and failure in pipelines. Hydrogen may activate defects that so far were dormant. The impact is linked to fatigue and addressed in the following sections of this chapter.

Fatigue

The aim of this section is to study the compatibility of natural gas/hydrogen gas mixtures with the offshore trunk lines regarding fatigue. The focus is on the influence that the hydrogen gas has on the fatigue properties of existing pipelines. First, a literature study is done, including the topics: hydrogen embrittlement, the sources of defects and inhibitor gases. This is followed by calculating the effect of hydrogen gas on the fatigue properties of two different pipelines as case studies.

Literature study

Hydrogen Embrittlement

Hydrogen embrittlement is defined as the embrittling of a metal due to exposure to hydrogen. It is a complex set of processes that are not yet fully understood. For hydrogen embrittlement to occur, the following three conditions have to be present:

1. Presence of hydrogen
2. A susceptible material
3. Stress

In this section, the focus will be on gaseous hydrogen inside a pipeline, made of API 5L X42 to API 5L X70 grade steel, under cyclic loading (fatigue).

A series of events needs to take place before the hydrogen is able to influence the fatigue behaviour of steel. An overview of the events involved is given in Figure 12. First, the gaseous hydrogen has to be transported in the crack tip region (1), followed by the physical adsorption (2) of the hydrogen. The dissociation of the gas molecule into two hydrogen atoms happens at the surface (3). The hydrogen has to enter the material for hydrogen embrittlement to happen, at which the hydrogen atom is transported from the surface to the bulk material (4), called absorption.

This is followed by the diffusion of the hydrogen atoms in the bulk material (5). This is stress-assisted diffusion, whereby the hydrogen atoms move to the region of high triaxial stresses. Such a region can be found just ahead of a notch or a crack tip at which the mechanism of hydrogen embrittlement happens.

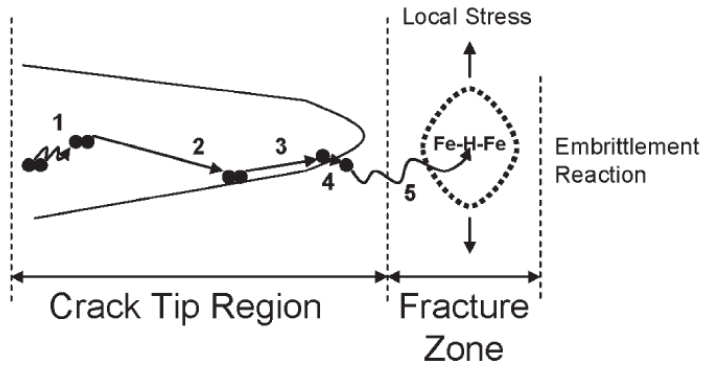


Figure 12: The series of events involved in hydrogen embrittlement [12].

Another phenomenon that may happen is trapping. Hydrogen is especially sensitive to this, because of its low solubility and high diffusivity in steel. The traps can be reversible or irreversible. Reversible trap sites have low binding energies. Examples of that are grain boundaries, dislocations and substitutional elements. On the other hand, irreversible traps have high binding energies, like second phase particles (e.g. carbides and oxides). The effective hydrogen concentration at the crack tip becomes lower if the hydrogen atoms are being trapped by irreversible traps, while reversible traps slow down the diffusion process. This lowered effective hydrogen concentration will reduce the severity of the hydrogen embrittlement. Hydrogen assisted fatigue crack growth (HA-FCG) is a complicated phenomenon involving many steps as described above. The rate-limiting step in this process depends on test parameters.

The hydrogen pressure influences the fatigue crack growth behaviour. Sievert's law describes the dissolved hydrogen concentration in steel under equilibrium conditions and is as follows:

$$C_H = k\sqrt{p_{H_2}}$$

Where C_H is the concentration of hydrogen in steel, p_{H_2} is the amount of pressure of the hydrogen gas and k is a constant. The dependency of the fatigue crack growth rate is found to be of the power 0.36 instead of 0.5 for X42 steel, $R = 0.25$, $f = 0.1$ and $\Delta K = 22 \text{ MPa}\sqrt{\text{m}}$. This dependency can be observed in Figure 13.

This lowered value for the exponent can be caused by multiple factors. The first factor is the irreversible trapping of the hydrogen atoms by impurities, which lowers the amount of free hydrogen in the metal. The second factor deals with the nonequilibrium concentration of hydrogen in the metal. No equilibrium is reached due to the dynamic testing, which gives the dissolved hydrogen too little time to reach an equilibrium state of concentration. This phenomenon depends on the time aspect of dynamic testing and is therefore linked to the frequency, which will be subsequently discussed.

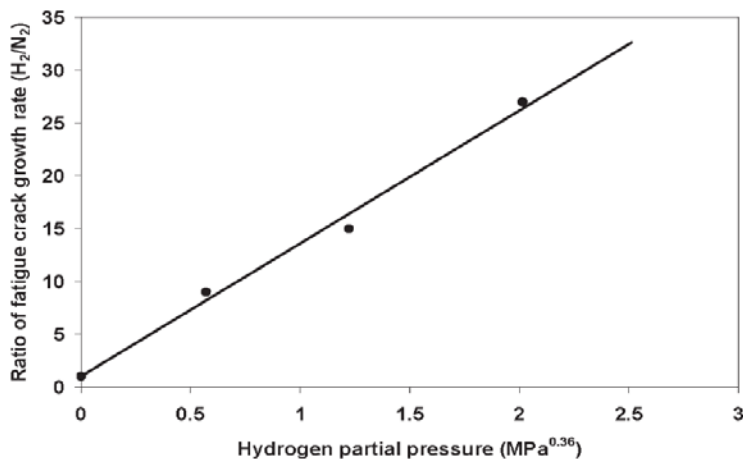


Figure 13: Crack growth rate versus hydrogen partial pressure for X42 steel, $R = 0.25$, $f = 0.1$ and $\Delta K = 22 \text{ MPa}\sqrt{\text{m}}$ [13].

The consequence of the higher crack growth rate with increasing pressure is that the amount of cycles to failure decreases. This can be observed in Figure 14. This testing has been done for X80 grade steel, which is not within the scope of materials for this section. However, this behaviour can also be expected for the X42-X70 grade steels.

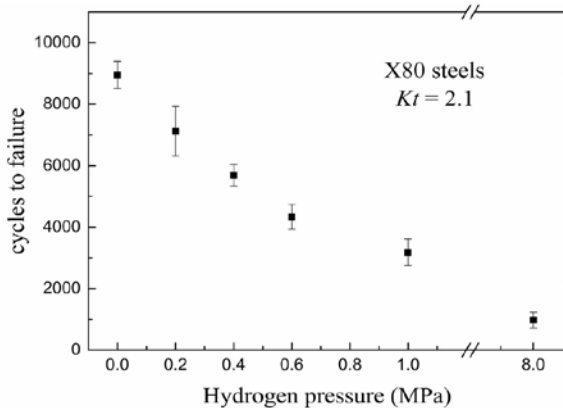


Figure 14: Cycles to failure versus hydrogen pressure for X80 steel under cyclic loading ($\Delta\sigma=636$ MPa) [14].

There is an effect of frequency on the fatigue crack growth, depending on the frequency range. Above 0.1 Hz, a dependency is found in several references [15], [16]. However below the frequency of 0.1 Hz, no dependency has been observed [17], [18]. The crack growth per cycle decreases with an increase in frequency. This is probably due to one of the rate-limiting steps in HA-FCG that is controlled by the frequency. These rate-limiting steps are: the rate of creation of a new crack surface, the rate of hydrogen dissociation and adsorption, and the rate of diffusion to the crack tip plastic zone. This indicates that a transport-limited phenomenon is present above the 0.1 Hz. Below the 0.1 Hz, an equilibrium of hydrogen transport is reached and therefore this will not be the rate-limiting step anymore. However, more research is needed to understand these rate-limiting steps and pinpoint the influence of frequency.

The EU-project Naturalhy (2004-2009) deals with the use of gaseous hydrogen in the existing pipelines and, more specifically, with the hydrogen enhanced fatigue crack growth in work package 3 [19]. The material range X42 to X70 were tested and the results are given in Figure 15.

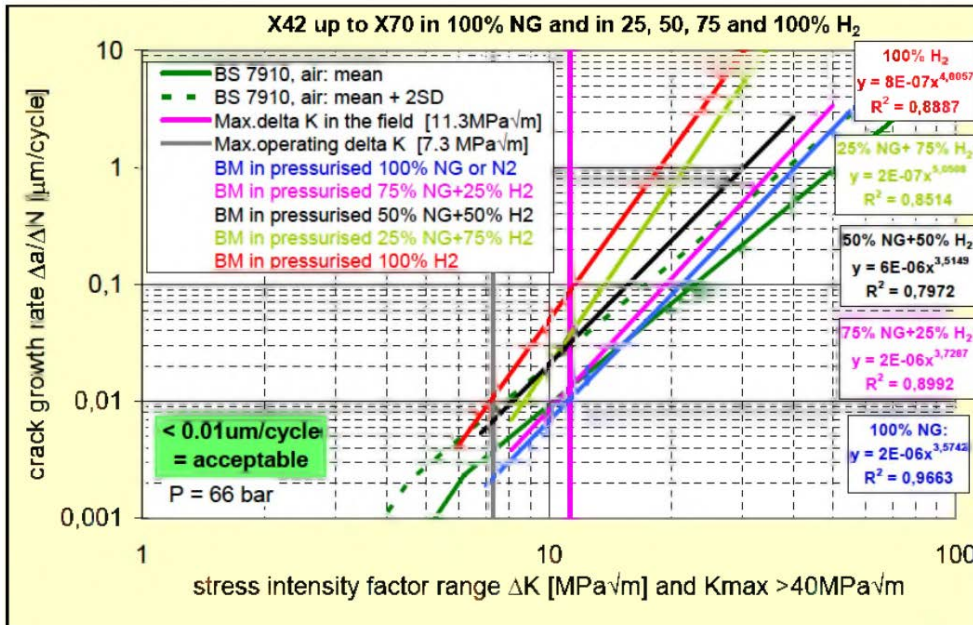


Figure 15: Crack growth rate versus stress intensity factor range [19].

Naturally also studied the fatigue properties of the base and weld material. There is no difference observed between the fatigue behaviour of the base and weld materials. Thus, the weld material has the same fatigue properties; however, it might be more prone to crack initiation by weld defects or other damage mechanisms. This will be discussed in the next part.

Sources of defects

The presence of defects in the material is crucial for the initiation of fatigue cracks. The most critical criterion is the stress put on the material by a defect, which is described by the stress intensity factor. The shape of the defect influences the stress intensity factor. Blunt defects, like corrosion, lead to low stresses, while sharp defect may cause high stresses. These sharp defects are often cracks or crack-like defects, and they have a higher probability of growing under fatigue loading. Therefore, cracks and crack-like defects are considered to be more critical than e.g. corrosion defects.

Weld defects are crack-like defects and need to be considered in this research. Another source of cracks is caused by stress corrosion cracking (SCC), which is a case of environmentally assisted cracking. Stress corrosion cracks are often transgranular and are therefore sharp defects. The outer surface of the pipeline may be subjected to SCC due to the chemistry of the soil, especially if a coating is applied, as it may result in an extreme local environment caused by coating failure. These cracks will exist at the outer surface of the pipeline, as shown in Figure 16. Most cracks due to SCC become dormant, but they might be initiation sites for fatigue cracks. Also pitting corrosion may result in defects having high stress concentrations, if these pits are both narrow and deep. Shallow pits are not a major concern, and may be considered as a reduction of wall thickness.

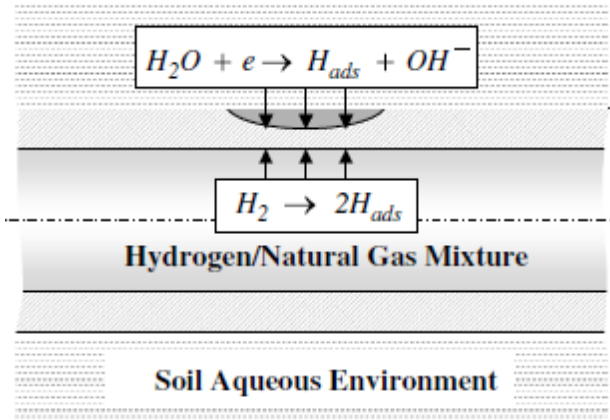


Figure 16: Crack at the outer surface of the pipeline, due to SCC [20].

Inhibitor gases

The addition of small concentrations of certain gases to hydrogen may slow down the effects of hydrogen assisted fatigue crack growth or even stop the entire process. These gases adsorb to the steel specimen, but do not diffuse into the bulk material. They are blocking the adsorption of hydrogen at the surface and therefore fewer hydrogen atoms can diffuse into the bulk material. Gases containing C, S and O block the hydrogen adsorption by forming semi-stable bonds with iron on the surface and are called inhibitor gases. The gas that shows the most potential is O_2 [21].

In NaturalHy, oxygen is used to determine the effectivity of using inhibitor gases. Figure 17 shows the effect oxygen has on the crack growth rate in a 100% gaseous hydrogen environment. The test starts without the addition of oxygen (red line) and it results in a crack growth rate of $4.56 \mu\text{m}/\text{cycle}$. Followed by the addition of 250 ppm O_2 (yellow line), when immediately the crack growth rate is reduced to $0.17 \mu\text{m}/\text{cycle}$. The crack growth rate is further reduced by adding more oxygen. By adding 500 ppm O_2 (grey line), the crack growth rate is negligible with a value of $0.05 \mu\text{m}/\text{cycle}$. After removing the oxygen, the crack growth rate increases again, but is less than before adding oxygen. Possibly, some oxygen remains present on the crack surface. This experiment shows the effectiveness of oxygen as an inhibitor gas.

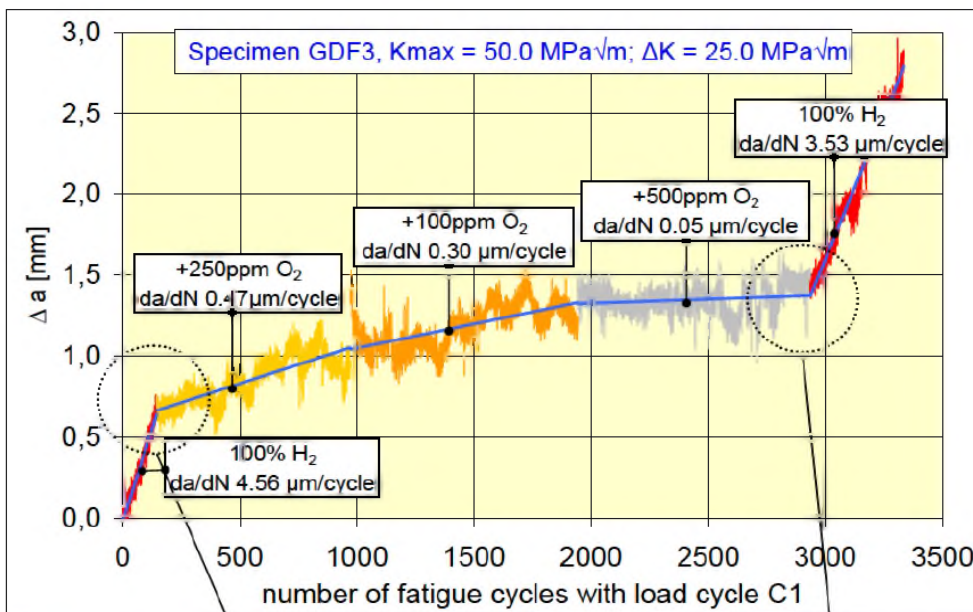


Figure 17: Crack growth versus number of fatigue cycles, with oxygen added in various amounts [19].

Fatigue calculations

The results of the survey summarized above are used to determine the number of cycles to failure for a pipeline subjected to fatigue. Two specific cases of pipelines currently operating in the North Sea have been selected. The assumed cyclic loads are the result of pressure swings due to (i) daily packing of the pipeline or (ii) yearly depressurization to atmospheric conditions. These assumptions are very conservative and not in line with current practice, but valid from a worst-case analysis perspective. An initial crack geometry is assumed in line with what can be detected by non-destructive testing.

The calculations followed can be found in Appendix A. It is concluded that, for either case analysed, in the case of daily pressure swings, the crack (assumed) is not expected to grow. In case of yearly full depressurization cycles, the crack can grow, but it will take an elevated number of cycles (years) to do so. Fatigue is therefore not found to be a critical failure mechanism for the offshore pipeline analysed.

Outlook

In this section, the compatibility of natural gas/hydrogen gas in the existing offshore trunk lines is studied. The focus is the influence of gaseous hydrogen on the fatigue properties of steel and the resulting crack propagation. So far, no showstoppers have been identified. Assuming a critical crack size that is invariant of hydrogen exposure, no significant effects due to hydrogen-enhanced fatigue crack growth is expected with the current parameters and boundary conditions. This approach and parameters are solely applicable to the materials range X42-X70. It is noted once more that the current status of the pipelines has been left outside the scope of this investigation. It is recommended to use the results contained in this report with the results of an inspection, that determines whether defects exist and whether those match the assumptions taken in this investigation.

The assumption made of a small amount of fatigue crack growth (only 0.15 mm) means that only a small amount of fatigue crack growth will result in considerable remaining life. This intuitively gives some evidence that these pipelines would be safe for hydrogen use for the foreseeable future. However, it should be checked that they don't become so brittle from hydrogen that even limited or no fatigue crack growth could result in crack growth.

It should also be verified that the crack growth rate da/dt is also negligible relative to the service life by calculation of a da/dt vs K analysis or that the applied stress intensity is below the threshold for environmentally assisted crack growth.

Hydrogen enhanced fatigue crack growth in pipes is mostly influenced by the following three parameters: pressure, material and frequency. Both the material and frequency are fixed for the existing pipeline network. Therefore, the pressure is the parameter that needs to be taken into account for reusing the pipelines. A safe operating window can be determined by integrity management, of which an example is given in Figure 18. The concept is to calculate the allowable initial crack length as a function of the applied pressure. This initial crack length is derived from a maximum crack length (a_{max}), which is allowed to be present at the end of the chosen design life. The maximum crack length may be the critical crack length at which unstable crack growth occurs or a chosen value that is lower than the critical crack length (as done in this report). The resulting initial crack lengths depend on the maximum crack length, the percentage of hydrogen in the gas mixture and the chosen design life. The cracks should be measured at the beginning of the time period. In the existing offshore trunk lines, this can be done by non-destructive inspection. The inspection interval may be considered as the chosen design life. Also, other parameters can be implemented in the evaluation, i.e. reduction in wall thickness in time.

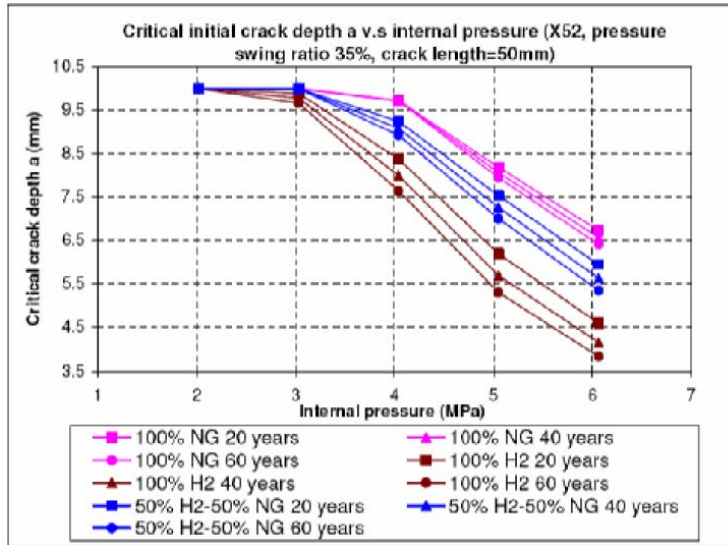


Figure 18: Critical crack depth versus internal pressure, to determine a safe operating window [23].

4 Compressors: impact of H₂

Compressors are the heart of any gas transport infrastructure. In the North Sea, compressors are used to boost the gas streams towards the shore. Compressors are also used to reduce the wellhead pressure, thus increasing the recovery rate of the hydrocarbon reservoir. As the reservoir pressure declines throughout its life, compression becomes attractive to asset developers to continue elevated production rates, even at the cost of investing in new (or revamped) equipment and energy costs to drive the units.

In the North Sea, compression is applied with two different technologies:

- Reciprocating compressors
- Centrifugal compressors

In general, it can be stated that centrifugal compressors are the preferred choice when large volumes of gas need to be compressed [24]. For smaller volumes, reciprocating compressor technology is favoured due to its better efficiency and flexible operation. Reciprocating compression technology typically requires more maintenance and creates more noise and mechanical vibrations.

In a future service for the North Sea infrastructure in which hydrogen is to play a role, compressors will continue to be the heart of the export system. In the basis of the assessment described in chapter 2, a compressor operating with a blend of natural gas and hydrogen is considered, but also with only hydrogen. Therefore, it is of interest to understand whether compressors could potentially be re-used for hydrogen duty (or a blend of natural gas and hydrogen). If new units were to be required, it is important to have an estimate of the cost of such machines.

Reciprocating compressors

A proven method to compress hydrogen is to use reciprocating piston compressors. Widely used in refineries, they are the backbone of refining crude oil. Reciprocating piston compressors are commonly available as either oil-lubricated or non-lubricated. For high purity end-use standards (such as fuel cells), non-lubricated compressors (often called *dry*) are preferred to avoid oil contamination of the hydrogen. Reciprocating compressors offer excellent flexibility in handling gases with different molecular weights, though gases with a very low value (such as hydrogen) require additional attention on seals. One of the drawbacks associated with this type of compressors is their high maintenance cost because of wearing components such as valves, rider bands and piston rings [25]. Nevertheless, professional know-how on piston sealing and packing rings can guarantee that reciprocating compressors outperform competing technologies in terms of operational expenses.

If a reciprocating compressor was to be re-used for hydrogen service, the following aspects should be analysed in detail:

- Compatibility of the materials in contact with hydrogen, at local pressure and temperature conditions,
- effect on performance and operational envelope,
- acceptability of hydrogen stream contamination with lubricant,
- acceptability of fugitive losses through the seals.

Though no particular study has focused on evaluating the actual tolerance of this type of machine to hydrogen concentration, values up to 10%vol have been claimed not to be critical [26].

Centrifugal compressors

Centrifugal compressors in the energy sector are tailor-made machines for every specific project. Their aerodynamic design is a compromise between peak aerodynamic efficiency at a given design point and the breadth of the operational envelope together with the efficiency at off-design conditions. As such, they are sensitive to the fluid properties of the process stream. Existing compressors can even be rebundled with new impellers as the asset matures to retune the maximum efficiency to the new normal operating conditions.

The design of centrifugal compressors is determined by the flow rate, the thermodynamic properties of the gas and the required pressure ratio [1]. The low density and molecular weight of hydrogen poses a challenge

to centrifugal compressor designers, as the impeller tip speed needs to be very high to achieve a reasonable pressure ratio. From a structural standpoint, this is difficult to achieve, which can lead to a selection of a high-strength alloy which may not be compatible with high concentrations of hydrogen [2]. In particular, hydrogen embrittlement in the heavily-loaded impellers can result in unacceptable levels of safety. In applications in which centrifugal compressors currently handle high concentrations of hydrogen (hydrogen recycle in refinery, or syngas, for example), the design is based on long shafts with a large number of impellers [27].

If a centrifugal compressor was to be re-used for hydrogen service, the following aspects should be analysed in detail:

- Compatibility of the materials in contact with hydrogen, at local pressure and temperature conditions,
- effect on performance and operational envelope,
- acceptability of hydrogen stream contamination with lubricant,
- acceptability of fugitive losses through the seals.

Re-use of existing natural gas centrifugal compressors for hydrogen service has been deemed *impractical* [28], though concentrations up to 10% vol have been claimed not to be critical [26]. In view of the demand to go to a large-scale transport of hydrogen and the difficulties mentioned, efforts are being made to optimize centrifugal compressor technology for pure hydrogen service [29].

Costs of replacing a compressor system for hydrogen duty

In this section, an initial exploration of the costs of replacing a compressor system for pure hydrogen duty is described.

Sizing of and operating conditions

It is assumed that the compressor unit receives the hydrogen stream produced by the electrolyzers. According to the current state of the art technologies, the electrolyser delivers a compressed output of around 15-25 bar for alkaline technology and approximately 35 bar⁸ for PEM electrolysis⁹. Regardless of which of these two technologies are being used, a compressor is needed to boost the hydrogen.

The following compressor specifications are analysed in order to obtain their economic parameters of CAPEX & OPEX:

- Piston or diaphragm (positive displacement);
- Stages: overall pressure ratio 1.5-3.0. 30 bar suction as exit from PEM and 60-80 bar discharge for pipeline transport;
- Flow rate: electrolyser capacity installed of fixed 1 MW, 10 MW, and 100 MW of electrolyser input to suggest flow rates. The equivalent flow rates at electrolyser efficiency of 55 kWh/kg H₂ is 18.2 kg/h, 182 kg/h and 1820 kg/h (~200 Nm³/h, ~2000 Nm³/h, ~20000 Nm³/h)
- Thermodynamic efficiency from the OEM catalogue.

Compression power

For the purpose of this study, a compression power denoted by \dot{W} , is calculated as follows [28]

$$\dot{W} = \dot{m} \cdot \frac{R T_1}{M_w} \cdot \frac{\gamma}{\gamma - 1} \cdot \frac{Z_1 + Z_2}{2} \cdot \frac{1}{\eta_s \eta_m} \left[\left(\frac{P_2}{P_1} \right)^{\frac{\gamma-1}{\gamma}} - 1 \right]$$

where:

- \dot{m} the mass flow rate (in [kg/s])
- P the pressure of the compressor at suction (1) and discharge (2),
- Z the hydrogen compressibility factor at suction (1) and discharge (2),
- T the inlet temperature of the compressor (333.15 K),

⁸ Siemens, SILYZER 300 data sheet, Siemens, 2019.

⁹ Examples of different electrolysis technologies and their outlet pressure: Alkaline → [Hydrogenics HySTAT™](#) 15-25 barg, Etogas 15 bar, Tractebel 0-15 bar; PEM → [Siemens Silyzer 200/300](#) 35 bar, Tractebel 30-60 bar. It is expected that due to technological innovation, this may increase towards 60 barg.

- γ the specific heat ratio (1.4),
- M_w the molecular mass of hydrogen (2.016 kg/kmol),
- η_s the isentropic compressor efficiency (80% ¹⁰),
- η_m the mechanical losses from the driver (98%),
- R the universal constant of ideal gas $R = 8314 \text{ J/(K kmol)}$.

Economics

When assessing costs for mechanical equipment at a conceptual level, it is of vital necessity to rely on dependable and easy-to-use methods for estimating the main cost parameters, such as Capital Expenditures and Operational Expenses.

However, when faced with the situation of estimating compressor costs, diverse published methods turn out with significant differences in their projected results. Moreover, most of the literature uses a single parameter for cost estimation, which is the compressor power. Other references such as [30] consider the suction pressure along with the compressor power to estimate more accurately the compression costs.

Following again the insights from [31], the adopted ¹¹ compression CAPEX method relates in a linear way to the compression power:

$$CAPEX_{compression}[\text{€}] = 2,655.04 \times \dot{W}$$

The reason to follow this particular method is basically for being the most up-to-date one without needing to incur in more detailed basic engineering specifications. Please note that the CAPEX calculated by this formula includes the entire compressor package, i.e. driver and ancillary equipment.

With regards to the operational expenditures, after some private communications with compressor design manufacturers, the recommendation is to consider 8% per year for planned maintenance on average over 15 years. The reason behind it is to account for piston rings, guide rings, valves and packings needed to be replaced after several running hours repeatedly. After 40,000 hours also the frame with bearings and crossheads, among other parts, needs to be checked. Lastly, for a running period of 15 years, one replacement of pistons, cylinder liners, crosshead liners and crossheads are considered as well.

The annual maintenance fee of 8% of the CAPEX is added to the electricity costs to estimate the total annual cost of running the compressor skid:

$$OPEX_{compression} = (A_0 \times H_{year} \times e/DTE) \times \dot{W} + 0.08 \times CAPEX_{compression}$$

where:

- A_0 Availability (85%),
 H_{year} Hours per year (8760h),
 e the electricity costs (0.06 €/kWh),
 DTE the Driver Thermal Efficiency (90%).

Results

After applying the compressor's specifications to the equations above, the following CAPEX and OPEX results are obtained for the three given flow rates:

\dot{m} [kg/h]	Power [kW]	CAPEX	OPEX
18.2	9.41	€ 24,982	€ 6,669
182	94.10	€ 249,826	€ 66,695
1820	940.95	€ 2,498,266	€ 666,950

¹⁰ From OEM catalogues.

¹¹ According to the European Central Bank consumer price index, today's prices in 2019 are 4.32% higher than average prices throughout 2014. The euro experienced an average inflation rate of 0.85% per year during this period. Therefore, 2,655.04 EUR is today's equivalent for 2,545 EUR in 2014.

Comparing these values against what was received as budget quotes from vendors, the following is obtained:

<i>Power [kW]</i>			
<i>Q [kg/h]</i>	18.2	182	1820
Own calculations	9.41	94.10	940.95
Vendors	12.00	100.00	900.00
<i>Variance</i>	22%	6%	-5%

<i>CAPEX [EUR₂₀₁₉]</i>			
<i>Q [kg/h]</i>	18.2	182	1820
Own calculations	~ € 25,000	~ € 250,000	~ € 2,500,000
Vendors	€ 200,000	€ 600,000	€ 3,000,000
<i>Variance</i>	88%	58%	17%

The results show quite a discrepancy between what is calculated using the chosen methodology against what the vendors inform in their budget quotes. Both, the compressor power and the compressor CAPEX tend to deviate from their vendors' counterparts with a percentage spread that decreases while the flow rate gets higher, which from a commercial perspective, such as the vendors', makes sense.

These differences are the result of adopting stochastic methods to estimate techno-economical parameters, which for a project at this conceptual stage are reasonable and expected. The estimations are based on limited information and subsequently, have relatively wide accuracy ranges. However, these ranges are accepted and typically used for project screening, determination of feasibility, concept evaluation, and preliminary budget approval, which are the overall objectives of this study¹².

The final recommendation is to use the values found above as indicative of what can be expected. For more accurate estimations, a more detailed basic engineering for a given asset is necessary.

Outlook

New developments are being carried out to advance High-Pressure Electrolysis (HPE) technology, which is based on PEM electrolysis, but with the difference that the compressed hydrogen output is around 120 to 200 bar at 70 °C. This technology can be very attractive since the cost of compression can be a substantial factor in the overall costs of any hydrogen-based energy storage pathway. Vendors are also pursuing such technology, and there are currently R&D projects devoted to this end.

¹² The expected accuracy of this sort of estimates ranges between -15% to -30% on the low side, and +20% to +50% on the high side, depending on the technological complexity of the project, appropriate reference information, and the inclusion of an appropriate contingency determination. This estimate refers to those classified as a Class 5 or 4 by the *American Association of Cost Engineering* (AACE) and a Budget estimate (typically -15% to + 30%) by the ANSI Standard Reference Z94.2-1989.

5 Gas engines and gas turbines: impact of H₂

In the overview of equipment in contact with H₂ described in chapter 2, it has been identified that combustion equipment may receive a mixture of natural gas and hydrogen, depending on whether or not hydrogen is admixed upstream of off-take of fuel gas. The affected equipment concerns mostly prime movers such as gas turbines, gas engines or gensets, but potentially also gas-fired heaters. This scenario is therefore rather hypothetical.

This chapter offers a short summary of the issues identified by other researchers when it comes to introducing hydrogen-natural gas blends to existing gas turbines or gas engines.

Gas engines: impact of Hydrogen additions

It is possible to add up to 2 %vol hydrogen for all motors [32]. Above 2 %vol, additional management systems are required to cope with the fluctuations in hydrogen concentration. These fluctuations can cause engine knocking, generation of NO_x and engine wear. Modern systems may be able to control the fluctuations. The engine could potentially deal with concentrations up to 10%, if the methane number remains above the minimum (70). In general the performance of gas engines' efficiency is improved, because flame speed is increased and reactivity is higher [33].

Gas turbines: impact of Hydrogen additions

In general, the most challenging issue when adding hydrogen to natural gas is the generation of exhaust gas NO_x in gas turbines [34], [35], due to an increase in adiabatic flame temperature. When a lean mixture is used, less NO_x can be expected, but the generated power decreases due to the reduction in heat rate. Without any adjustments, 1 %vol hydrogen can be added to gas turbines [36]. Most turbines can even use 1-5 % hydrogen or need minor adjustments to do so. Up to 10%vol hydrogen can be fed to the gas turbines with modifications and tuning. Newer turbines may be equipped to handle 15%. There are special designed syngas turbines that can handle up to 50% concentration of hydrogen.

In terms of controlling the combustion process, the biggest technical challenge due to the addition of hydrogen is an increase in flame speed [36]. The flame speed of pure hydrogen is 10 times larger than natural gas, and therefore there is a higher chance of flashback. The concentration limits at which hydrogen is flammable are wider than for natural gas, which is positive as hydrogen can be burned for a lean premixed combustion. However, a higher risk of unwanted combustion is created. When using a catalytic converter, NO_x generation can be decreased to very low levels [37]. Further research is required to generate knowledge on start-up, flame stability and emission issues.

More recently, a test of a new large scale gas turbine (700 MW) showed promising results with 30% hydrogen. Due to premixing, the NO_x exhaust could be reduced and 10% reduction of CO₂ emission. Tests on smaller gas turbines (25 – 53 MW) with premixed systems show that it is possible to add 15-40% hydrogen with only small adjustments in the turbines [36]. These systems do not exceed 24 ppm NO_x emission. Small gas turbines below 25 MW can operate with hydrogen with little or no adjustments .

At present, most gas turbine vendors are in the process of developing retrofit solutions to accommodate higher concentrations of hydrogen, or to have hydrogen-ready machines available in their portfolio.

6 Flow meters: impact of H₂

In this chapter, the impact of hydrogen on flow meters is described. The chapter is divided in two sections: first, a summary of literature is offered; second, information received from vendors is summarised.

Literature survey

Due to the addition of hydrogen to natural gas, the physical properties of the gas mixture will change. At the same conditions of pressure and temperature, a natural gas composition containing hydrogen will experience the following variations in fluid properties:

- Gas density is reduced
- Dynamic viscosity is reduced (small effect)
- Velocity of sound is increased
- Reynolds number is reduced (at similar flow speed)
- Calorific value is reduced.

As explained already in chapter 3, the ratio of the calorific value of methane to the calorific value of hydrogen amounts to 3. This means that for transporting the same energy flux, the gas velocity should increase with a factor 3. It will be discussed below why this factor cannot be achieved yet by existing gas flow meters. Reference [38] has studied the effect of the additions of hydrogen on metering errors and uncertainties in volume (flow) measurement by setting up an uncertainty budget model. Mixtures of natural gas and hydrogen increase the measurement error and metering data uncertainties. Billing values become less accurate. Measurement errors increase with increasing concentrations of hydrogen.

Three types of measuring principles used in industry have been considered in this study: turbine meters, ultrasonic meters, and Coriolis meters.

Turbine flow meters

The measuring principle of a turbine meter is based on turning a turbine wheel by the gas flow. The rotational speed of the wheel is proportional to the flow speed and the actual flow rate. An interesting parameter for the flow measurement of blends of natural gas and hydrogen with turbine meters is the maximum gas velocity. According to current product specifications, the maximum actual flow rate amounts to 24000 m³/h for a bore diameter of 600 mm (maximum size). This maximum flow rate is valid for *all* type of gases, regardless of their composition. Consequently, the maximum velocity amounts to approximately 24 m/s. The maximum velocity is limited as the mechanical parts of the turbine meter may be damaged by applying higher gas flow velocities. Also, erosion can be a problem for turbine meters because of the velocity of the particles potentially transported with the gas. These will be able to degrade the surface of the rotating wheel. Therefore, for transporting the same amount of energy by natural gas-H₂ blends or 100% hydrogen, velocities larger than ~24 m/s are needed (assuming the line operates at capacity with natural gas).

Additions of hydrogen to natural gas will have an effect on the measuring principle of the turbine flow meters. A relevant parameter is the minimum energy in the flow needed to drive the turbine wheel. This is determined by the minimum flow rate and the actual gas pressure. The minimum pressure should be maintained as per manufacturer specifications. Following hydrogen additions, the minimum flow rate should be increased. Consequently, the measuring range in actual flows is reduced when hydrogen is introduced to the natural gas mixture.

Research & Development is performed now by the manufacturers to investigate the suitability of turbine meters for measuring higher gas velocities (> 25 m/s). Most manufacturers now state that the current turbine meters are suitable for a maximum of 10 vol% of hydrogen.

Ultrasonic flow meters

The measuring principle is based on the measurement of the time difference of ultrasonic signals travelling with, and in opposite direction, of the gas flow. The gas velocity and actual volume flow rates are both proportional to the time difference between these two measurements. Regarding the maximum flow velocity achievable by existing flow meters, a maximum actual flow rate of 30000 m³/h for a bore diameter of 600 mm (maximum size) is currently specified for this type of meters. This maximum flow rate is valid for *all* type of

gases regardless of their composition. Consequently, the maximum velocity amounts to approximately 29 m/s, which is again insufficient to transport the same amount of energy in hydrogen as it is currently done with natural gas. Higher flow velocities will lead to issues with the measuring principle, as the ultrasonic signal from the sending sensor may be unable to reach the receiving sensor, and instead hit the spool wall. Additions of hydrogen to natural gas also have another effect on the measuring principle. The ultrasonic signals are disturbed since, as higher concentrations of H₂ are introduced, the speed of sound is increased and the signal-to-noise ratio is reduced, leading to larger measurement uncertainties.

Manufacturers of ultrasonic meters are performing R&D on the topic of ultrasonic signal path layout and frequency, destined to develop ultrasonic meters suitable for natural gas-hydrogen blends. Most manufacturers now state that the current ultrasonic meters are suitable for a maximum of 10 vol% hydrogen.

Coriolis flow meters

The measuring principle is based on the Coriolis principle. Two pipe elbows are vibrated by means of actuators. Sensors are mounted near the inlet and the outlet of the oscillating system to detect the vibration signals. Without flow, both signals are in phase. A phase shift between the two signals develops as gas is flowing through the device, resulting from the Coriolis force on the moving fluid. The phase shift is proportional to the mass flow.

Addition of H₂ to natural gas does *not* have an effect on the measuring principle itself. At higher volume concentrations of hydrogen (at the same velocity) the phase shift will be smaller. Coriolis meters are suitable for measuring the gas flow of 100 vol% hydrogen. For the same amount of energy transported, gas velocities need to be significantly higher. The risk of erosion will be increased if high velocities are achieved. It should be noted that the measurement uncertainty is dependent on the ratio of the mass of the fluid inside the vibrating tubes and the mass of the tubes themselves. With hydrogen, this ratio is less favourable due to the lower density of hydrogen.

Miscellaneous

Other issues are identified in literature when existing gas flow meters are intended for service with hydrogen (or concentrations thereof), which are not directly related to the measurement itself:

- Gas leakage
- Material embrittlement
- Shortening the service life
- Lubrication (type and frequency of lubrication)
- Metrological approval not including 100% hydrogen
- Wet calibration of high-pressure flowmeters using hydrogen as flowing medium is not possible

Flow rate measurements are most typically used for billing purposes, but also for process control. Billing is proportional to the (i) flow rate only and (ii) the gas composition, and thus its calorific value. The gas composition is determined can be determined by a process gas chromatograph. Measurement of concentrations of hydrogen in a process gas chromatograph can be challenging. Process gas chromatographs often use a Thermal Conductivity Detector which measures the thermal conductivity of the gas components separated in the separation column. Helium is often used as a carrier gas. The thermal conductivity of Hydrogen differs not much from that of helium. Consequently, the sensitivity level is reduced if low Hydrogen concentrations are involved. Only limited values of hydrogen concentrations can be measured. A solution could be using another carrier gas, e.g. argon. Manufacturers of process gas chromatographs are performing more R&D developing gas chromatographs measuring a wider range of concentrations of Hydrogen.

The actual gas volumes are converted to standard gas volumes for billing purposes. An important gas property for this conversion is the gas compressibility. The gas compressibility is calculated using the AGA 8 [39], SGERG [40] and GERG 2004 [41] algorithms. The AGA 8 algorithm can be used for a maximum 10 vol% hydrogen. This is also valid for the SGERG algorithm. For higher volume concentrations, the algorithms should be reconsidered.

Input supplied by vendors

Vendors of flow metering equipment have been contacted to supply input regarding the admissible levels of hydrogen in a high-pressure stream. A total of four vendors have supplied input. A summary of the results is given below.

- **Vendor A.** No detailed information is available now. A public announcement is to be expected within a few weeks from the date of writing this report.
- **Vendor B.** Vendor B has provided custody transfer measurement system with an ultrasonic meter and flow computer to be used for the measurement of 100 vol% Hydrogen. There is no detailed information available about the process of gas flow measurement (confidential). In a second project, Vendor B has delivered a Coriolis mass flow meter used for 100 vol% hydrogen over a wide flow rate range and high accuracy. There is also no detailed information available about the process of gas flow measurement (confidential).
- **Vendor C.** Vendor C is a manufacturer of turbine meters and ultrasonic meters. According to vendor C, turbine flow meters exist that are suitable for 100 vol% hydrogen, but with reduced flow range. The materials are also selected to be suitable for 100 vol% hydrogen. Vendor C currently also supplies ultrasonic flow meters for gas streams with a hydrogen concentration up to 25%vol, but with reduced flow range. The metrological approval is not available for 100%vol H₂, but it is achieved for concentrations up to 50%vol H₂.
- **Vendor D.** Vendor D is a manufacturer of Coriolis meters and has a long track-record in metering streams of pure Hydrogen. Above a pressure of 40 bar the results are satisfactory. Below 40 bar, measuring hydrogen flow is quite challenging, because of the low gas density. Maximum velocities are up to 400 m/s; however, erosion could be a problem. One limitation is the allowed pressure drop in the system. The sizes in which the product is available range from 1.5 mm to 30 cm flange sizes.

7 References

- [1] "North Sea Energy Atlas," 2019. [Online]. Available: <https://www.north-sea-energy.eu/index.html>.
- [2] PBL, "Ontwerp van het klimaatakkoord," 2018.
- [3] J. P. van Soest and H. Warmenhoven, "Waterstof in het klimaatakkoord," 2019.
- [4] J. Matthijssen, E. Dammers, and H. Elzenga, "The future of the North Sea. The North Sea in 2030 and 2050," 2019.
- [5] M. T. Dröge and R. Kenter, "Gas pipeline incidents: 10th Report of the European Gas Pipeline Incident Data Group (period 1970 – 2016)," 2018.
- [6] E. Sletfjerding, J. S. Gudmundsson, and K. Sjøen, "Friction factor in high-pressure gas pipelines in the North Sea," in *Society of Petroleum Engineers - SPE/CERI Gas Technology Symposium 2000, GTS 2000*, 2000.
- [7] S. Mokhatab and W. Poe, *Handbook of Natural Gas Transmission and Processing*. 2012.
- [8] N. González-Díez, "Boosting the Energy Transition." TNO, Delft, 2019.
- [9] Energy Institute, "Guidelines for the Avoidance of Vibration Induced Fatigue Failure in Process Pipework," *Energy Inst.*, 2008.
- [10] M. Ho, S. El-Borgi, D. Patil, and G. Song, "Inspection and monitoring systems subsea pipelines: A review paper," *Structural Health Monitoring*. 2019.
- [11] B. P. S. C. San Marchi, "Technical Reference for Hydrogen Compatibility of Materials," 2012.
- [12] M. Gao and R. P. Wei, "A 'Hydrogen partitioning' model for hydrogen assisted crack growth," *Metall. Trans. A*, vol. 16, no. 11, pp. 2039–2050, 1985.
- [13] J. H. Holbrook, H. J. Cialone, M. E. Mayfield, and P. M. Scott, "The Effect Of Hydrogen On Low-Cycle-Fatigue Life And Subcritical Crack Growth In Pipeline Steels," Battelle Columbus Laboratories, Columbus OH, USA, 1982.
- [14] T. An, H. Peng, P. Bai, S. Zheng, X. Wen, and L. Zhang, "Influence of hydrogen pressure on fatigue properties of X80 pipeline steel," *Int. J. Hydrogen Energy*, vol. 42, pp. 15669–15678, 2017.
- [15] O. Vosikovskiy, "Fatigue crack closure in an X70 steel," *Int. J. Fract.*, vol. 17, no. 3, pp. 301–309, 1981.
- [16] H. F. Wachob and H. G. Nelson, "INFLUENCE OF MICROSTRUCTURE ON THE FATIGUE CRACK GROWTH OF A516 IN HYDROGEN.," in *Hydrogen Effects in Metals*, 1981, pp. 703–711.
- [17] R. J. Walter and W. T. Chandler, "CYCLIC-LOAD CRACK GROWTH IN ASME SA-105 GRADE II STEEL IN HIGH-PRESSURE HYDROGEN AT AMBIENT TEMPERATURE.," in *Effect of Hydrogen on Behavior of Materials*, 1976, pp. 273–286.
- [18] S. Yoshioka, M. Kumasawa, and M. Demizu, "Fatigue Crack Growth Behavior in Hydrogen Gas Environment," *J. Soc. Mater. Sci. Japan*, vol. 32, no. 355, pp. 435–440, 1983.
- [19] J. C. van Wortel, "Durability of steels for transmission pipes with hydrogen, EU-project 'Naturalhy' (WP-3), report no.: R0096-WP3-C-0, (D32)," 2019.
- [20] J. Capelle, J. Gilgert, I. Dmytrakh, and G. Pluvinage, "Sensitivity of pipelines with steel API X52 to hydrogen embrittlement," *Int. J. Hydrogen Energy*, vol. 33, no. 24, pp. 7630–7641, 2008.
- [21] N. Nanninga, A. Slifka, Y. Levy, and C. White, "A review of fatigue crack growth for pipeline steels exposed to hydrogen," *J. Res. Natl. Inst. Stand. Technol.*, vol. 115, no. 6, pp. 437–452, 2010.
- [22] J. C. C. Newman and I. S. Raju, "An empirical stress-intensity factor equation for the surface crack," *Eng. Fract. Mech.*, vol. 15, no. 1–2, pp. 185–192, 1981.
- [23] A. Krom and M. L. Zhang, "Knowledge of defect criticality, EU-project 'Naturalhy', (WP-4, Task B), (draft)," 2006.
- [24] P. Hanlon, *Compressor Handbook*. McGraw-Hill Education, 2001.
- [25] A. Witkowski, A. Rusin, M. Majkut, and K. Stolecka, "Comprehensive analysis of hydrogen compression and pipeline transportation from thermodynamics and safety aspects," *Energy*, 2017.
- [26] K. Altfeld and D. Pinchbeck, "Admissible hydrogen concentrations in natural gas systems," *Gas Energy*, 2013.
- [27] R. Kurz and K. Brun, *Compression Machinery for Oil and Gas*. 2019.
- [28] P. Castello, E. Tzimas, P. Moretto, and S. D. Peteves, "Techno-economic assessment of hydrogen transmission & distribution systems in Europe in the medium and long term," *Eur. Comm. Jt. Res. Cent.*, 2005.
- [29] F. A. Di Bella, "Development Of A Centrifugal Hydrogen Pipeline Gas Compressor," *Dev. a Centrif. Hydrog. pipeline gas Compress.*, vol. TM-1785, no. 1785, pp. 596–622, 2015.

-
- [30] W. L. Luyben, "Capital cost of compressors for conceptual design," *Chem. Eng. Process. - Process Intensif.*, 2018.
- [31] J. André, S. Auray, D. De Wolf, M. M. Memmah, and A. Simonnet, "Time development of new hydrogen transmission pipeline networks for France," *Int. J. Hydrogen Energy*, vol. 39, no. 20, pp. 10323–10337, 2014.
- [32] A. van der Noort, W. Sloterdijk, and V. M., "Verkenning waterstofinfrastructuur," 2017.
- [33] M. A. Escalante Soberanis and A. M. Fernandez, "A review on the technical adaptations for internal combustion engines to operate with gas/hydrogen mixtures," *Int. J. Hydrogen Energy*, 2010.
- [34] S. Taamallah, K. Vogiatzaki, F. M. Alzahrani, E. M. A. Mokheimer, M. A. Habib, and A. F. Ghoniem, "Fuel flexibility, stability and emissions in premixed hydrogen-rich gas turbine combustion: Technology, fundamentals, and numerical simulations," *Applied Energy*. 2015.
- [35] S. Taamallah, K. Vogiatzaki, F. M. Alzahrani, E. M. A. Mokheimer, M. A. Habib, and A. F. Ghoniem, "Erratum to 'Fuel flexibility, stability and emissions in premixed hydrogen-rich gas turbine combustion: Technology, fundamentals, and numerical simulations' [Appl Energy 154 (2015) 1020–1047](S0306261915004997)(10.1016/j.apenergy.2015.04.044)," *Applied Energy*. 2018.
- [36] J. Larfeldt, M. Anderson, A. Larsson, and D. Moell, "Hydrogen Co-Firing in Siemens Low NO X Industrial Gas Turbines," *Power-Gen Eur.*, 2017.
- [37] P. Chiesa, G. Lozza, and L. Mazzocchi, "Using hydrogen as gas turbine fuel," *J. Eng. Gas Turbines Power*, 2005.
- [38] K. Steiner, "Metering errors of residential meters and uncertainties of meter readings in case of injection of hydrogen into the natural gas network," vol. 2018, 2018.
- [39] J. L. Savidge and K. E. Starling, "Compressibility Factors of Natural Gas and Other Related Hydrocarbon Gases," 1992.
- [40] M. Jaeschke *et al.*, "Accurate prediction of natural gas compressibility factors by the GERG virial equation," 1988.
- [41] O. Kunz, R. Klimeck, W. Wagner, and M. Jaeschke, "The GERG-2004 wide-range equation of state for natural gases and other mixtures," in *GERG TM15*, vol. 6, Fortschritt-Berichte VDI, 2007.
- [42] B. R. MacKenzie and D. Schiedek, "Long-term sea surface temperature baselines-time series, spatial covariation and implications for biological processes," *J. Mar. Syst.*, 2007.
- [43] American Petroleum Institute, "Recommended Practice for Design and Installation of Offshore Production Platform Piping Systems," *Am. Pet. Inst. Recomm. Pract. 14E*, 1991.

8 Appendix A – Fatigue calculations

In this appendix, specific fatigue calculations for a hypothetical propagation of a crack in a North Sea pipeline are shown. The main parameters and assumptions are discussed. The results of the calculations are offered for two actual examples of pipelines in the North Sea.

Stress intensity factor

The stress field in the vicinity of a crack in the material is described by the crack intensity. The crack intensity is dependent on the crack size, the applied load and the geometry of the specimen and the crack. The general equation of this parameter is as follows:

$$K_I = f(\text{geometry})\sigma\sqrt{\pi a}$$

Where $f(\text{geometry})$ is the geometry factor, σ is the applied load and a is the crack size. The crack geometry applied in this research is given in Figure 19. A semi-elliptical surface crack is used with a finite thickness and an infinite width. The crack is positioned in the longitudinal direction of the pipeline. The equation for the stress intensity factor for the semi-elliptical surface crack [22] is as follows:

$$K_I = \sigma \sqrt{\pi \frac{a}{Q}} F\left(\frac{a}{B}, \frac{a}{c}\right)$$

Where

$$Q = 1 + 1.464 \left(\frac{a}{c}\right)^{1.65}$$

$$F = \left\{ C_1 + C_2 \left(\frac{a}{B}\right)^2 + C_3 \left(\frac{a}{B}\right)^4 \right\} C_4$$

$$C_1 = 1.13 - 0.09 \frac{a}{c}$$

$$C_2 = -0.54 + \frac{0.89}{0.2 + a/c}$$

$$C_3 = 0.5 - \frac{1}{0.65 + a/c} + 14 \left(1 - \frac{a}{c}\right)^{24}$$

$$C_4 = 1 + \left\{ 0.1 + 0.35 \left(\frac{a}{B}\right)^2 \right\} (1 - \sin \varphi)^2$$

The stress (σ) applied on the material by a crack is the superposition of the pressure in the pipeline on the pipeline wall and the hoop stress of the pressure on the crack itself, described in the following equation:

$$\sigma = P \left(1 + \frac{R}{B}\right)$$

Where P is the pressure inside the pipeline, R is the radius of the pipeline and B is the wall thickness.

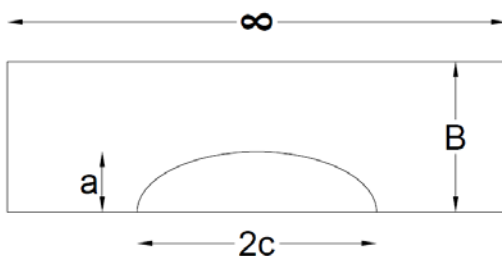


Figure 19: Crack geometry of the semi-elliptical surface crack on the inside of a pipeline in the longitudinal direction.

Fatigue: Paris' law

The effect of fatigue is described in Paris' law. This equation gives the rate of growth of a fatigue crack and is as follows:

$$\frac{da}{dN} = C\Delta K^m$$

Where

da/dN	the crack growth (da) per loading cycles (N)
ΔK	crack intensity range, defined as $\Delta K = K_{\max} - K_{\min}$
C	constant,
m	constant

The results of NaturalHy, given in Figure 15, are used in the calculations. Table 6 gives the results in tabular form. This table contains the parameters used in the Paris' law and also includes the threshold intensity factor (ΔK_{th}) with increasing hydrogen content. This is the stress intensity factor at which the fatigue crack starts growing. If the calculated stress intensity range is below this number, the crack will not grow due to fatigue.

Table 6: The results of NaturalHy for the fatigue calculations [19].

H ₂ (%)	Log ₁₀ C (-)	m (-)	ΔK_{th} (MPa \sqrt{m})
0	5.69	3.57	10.7
25	5.69	3.72	9.9
50	5.22	3.51	8.2
75	6.69	5.05	8.5
100	6.09	4.80	7.1

Boundary conditions

The parameters regarding the geometry of the crack are essential. The crack size is applied as a boundary condition in the calculations in this report. The crack width (c) is 25 mm and the crack depth (a) is 3 mm. These values are chosen, because as dormant defects these sizes are detectable by non-destructive inspection. The maximum allowable increase of the crack size is chosen to be 0.15 mm, which is a reasonable crack growth to stay on the safe side.

There are two types of pressure that need to be clearly distinguished from each other, because they influence the fatigue mechanism in a different way. The first is the total pressure (P) in the pipeline, or the pressure cycles (ΔP) in case of fatigue. This pressure determines the applied stress on the crack, used in the stress intensity factor calculation. The second pressure is the partial hydrogen pressure, which is the partial pressure that is caused by the addition of hydrogen. This pressure contributes to hydrogen embrittlement.

Pressure cycles will be used to determine the stress intensity range. Two different types of cycles are employed. The first is daily pressure cycles that may occur and is considered to be 20 bar. The second pressure cycle is in case of a sudden pressure drop and is considered to be 79 bar, from the operating pressure of 80 bar to atmospheric conditions of 1 bar. This sudden pressure drop is not expected to happen often and is considered to be yearly to be on the safe side.

In the literature study, the effect of frequency on the test results has been discussed. Since the frequencies of the pressure cycles are very low, this parameter is not expected to influence these fatigue conditions. The calculations are solely for the material range of X42-X70.

Case studies

Two case studies are presented in this section, applied to a 100% H₂ environment. The pipelines, called A and B, have dimensions corresponding to pipelines that can be found in the North Sea. The specifications of these pipelines are given in Table 7.

Table 7: The specifications of the case studies.

Pipeline	A	B
Wall thickness (mm)	11.6	35.0
Outer diameter (mm)	160	970
Material	API 5L X60	API 5L X60
Installed	~1980	~1980
Weld	Longitudinal	Longitudinal

The results of the case studies are given in Table 8. The boundary conditions described above have been put into the equations presented in this appendix. The outcome is that for the daily pressure cycle, no crack growth due to fatigue is expected because it represents a stress intensity range below ΔK_{th} . The pressure cycle of 79 bar has higher stress intensity ranges, which are higher than the threshold intensity factors for both cases. Pipeline A has the best results, being able to withstand at least 9000 cycles according to the calculations. Pipeline B also has good results, with 940 cycles until reaching the increase in crack length by 0.15 mm.

Table 8: Results of the case studies given in Table 7.

	Pressure cycle (bar)	ΔK (MPa \sqrt{m})	Above ΔK_{th}	da/dN ($\mu\text{m}/\text{cycle}$)	Cycles until a_{max} (-)
A	20	2.0	No	-	-
	79	7.5	Yes	0.017	9000
B	20	5.9	No	-	-
	79	12.6	Yes	0.16	940